



UBIQUITOUS FRACTAL DIMENSION OF OPTIMAL PATHS

By José S. Andrade, Jr., Saulo D.S. Reis, Erneson A. Oliveira, Eric Fehr, and Hans J. Herrmann

The fractal dimension of an optimal path in the strong disorder limit could be a fundamental property of many natural systems.

Searching for and characterizing a disordered landscape's optimal path is an important problem in theoretical and computational physics due to its often intimate association with relevant scientific and technological applications.^{1–4} In physics, the optimal path through a random energy landscape is important in explaining problems ranging from flow through disordered porous media to transport network navigation. In the latter case, the optimal path is crucial because it represents precisely the most efficient navigation strategy if global information about the underlying network topology is available.

As we describe here, the literature shows that the fractal dimension of an optimal path in the strong disorder limit appears to be a ubiquitous exponent for many physical models and related natural systems. We present detailed descriptions of three recent applications in which interfaces generated on 2D landscapes possess the same optimal path fractal dimension in the strong disorder limit. As our discussion shows, this fact poses new challenges to the field because the resemblance of all these fractal dimensions seems to hint at some deeper relation among the associated physical systems. This should be further investigated in the future from both theoretical and experimental points of view.

Optimal Path Issues

We start by defining a disordered landscape's optimal path. On an n -dimensional lattice, we assign to each site i a given energy value ε_i according to a probability distribution $P(\varepsilon)$. We then define the energy of any system path as the sum of all of its sites' energies. In particular, the optimal path between lattice sites i and j is the one among all paths connecting these two sites that has the smallest sum of all constituting sites' energies. This definition is somewhat similar to the definition of the shortest path in a network.⁵ In the well-known *brachistochrone problem* of classical mechanics, for example, the optimal path is related to the minimum energy path—that is, the path joining two points at which a falling particle travels the fastest from a higher to a lower point. In contrast, the shortest path of the brachistochrone problem is the straight line joining the two points—that is, the Euclidean space's geodesic.

Research has shown that optimal paths extracted from energy landscapes generated with weak disorder are self-affine and belong to the same universality class of directed polymers.⁶ In contrast, the strong disorder or ultrametric limit as studied by Marek Cieplak and his colleagues revealed the self-similar nature of the optimal path on 2D and 3D lattices with fractal dimensions given by $D_{opt} \approx 1.22$ and 1.43 , respectively.³ Surprisingly, the exponent value in two

dimensions is statistically identical to the fractal dimension found for disordered polymers ($\approx 1.2^3$), for strands in invasion percolation (IP; 1.22 ± 0.01^7), and for paths on minimum spanning trees (1.22 ± 0.01^8).

In the Cieplak study, they determine the fractality of the strong disorder limit's optimal path by associating the optimal path line with the minimum energy path on an isotropic two-dimensional lattice; this lattice is constructed by ranking bonds according to their energy values and removing the highest rank bonds thereafter. If removing a bond breaks the lattice connection, they keep the bond and remove the next ranked bond (if possible) and so on. Their results show that the optimal path ℓ scales with the lattice size L as $\ell \sim L^{D_{opt}}$ with $D_{opt} \approx 1.22$, defining a new universality class.

David Wilkinson and Jorge Willemsen introduced the IP model and its variants and used them extensively to simulate a non-wetting fluid's displacement through a porous medium by injecting a wetting fluid with different viscosity.⁹ Such a model has been very efficient when the injection process is quasi-static—that is, when it's in low velocity regimes. They then describe the displacement phenomenon using a cluster's growth on a lattice, assuming that its border (perimeter) represents the separation interface between the two fluids. Given its applicability, researchers have widely investigated the IP model to

determine its basic properties and improve its predictions for key practical problems. Two common IP process models are

- the *IP with trapping* (TIP) model and
- the *non-trapping* IP (NTIP) model.

These two IP model variants have been the focus of intense research, particularly because they exhibit self-organization into critical states.^{10,11}

The TIP model was originally devised to describe the invasion process of incompressible fluids in disordered porous media. As a microscopic rule, pore invasion is forbidden by the incompressibility constraint when the invaded fluid is completely surrounded by the invading one. In contrast, in the NTIP model, the displaced fluid is considered infinitely compressible and the injected fluid can penetrate into the fluid targeted for displacement through any of the separation interface's regions.

The NTIP model is implemented in several steps. Initially, we obtain a random value p_i from a uniform distribution in the range [0,1] and assign it to each network site i . At this point, the fluid to be displaced occupies all network pores, while the invading fluid is pushed through the inlet. Next, we search among the inlet's neighboring sites for the one carrying the smallest random number p . We invade this site and it becomes part of the region occupied by the invading fluid; we then update the list of sites eligible for invasion. The invasion process continues until the outlet is reached, when we can identify an invaded cluster providing global connection to the system.

In a later work, Cieplak and his colleagues introduced a novel

compressible IP model that forbids the occurrence of loops.⁷ Their results indicate that the IP strands have a fractal dimension of 1.22 in 2D and 1.43 in 3D. These strands, defined as the unique path that excludes dead ends from an arbitrary site to the central (injection) seed site, are therefore in the same universality class as optimal paths in the strong disordered limit.³ In two subsequent works, Markus Porto¹² and Stefan Schwarzer¹³ and their colleagues investigated other shared percolation process properties—beyond the self-similarity of TIP and NTIP clusters—including the shortest path between two points l , which should scale with the Euclidian distance r as $l \sim r^{D_{min}}$, where the

and subsequent re-crystallization processes that determine the multiple IP model's the continuous change of these self-similar structures. A similar situation is found in vulcanology: when magma is repeatedly injected through the same pathway, it always melts through the most recent formations to find its way out.¹⁵ For example, researchers have numerically investigated a pore structure's evolution after several invasion-frost-thaw events; the results indicate that the invasion clusters' fractal dimension varies with the number of invasion cycles if the porous pathway's structure is allowed to heal after each invasion occurs.¹⁶ In such situations—as well as in other cases of repeated

In the NTIP model, the displaced fluid is considered infinitely compressible and the injected fluid can penetrate into the fluid targeted for displacement through any of the separation interface's regions.

exponent D_{min} is the shortest path dimension D_{min} . From their numerical findings in 2D lattices—namely, $D_{min} \approx 1.13$ for NTIP, and $D_{min} \approx 1.21$ for TIP—it's possible to conclude that the shortest TIP path belongs to the same universality class as the optimal path in strong disordered energy landscapes.

Multiple Invasion Percolation

Under a different framework, Ascânia Araújo and his colleagues investigated a multiple IP model to simulate corrosion and intrusion processes.¹⁴ Inspired by the fact that gem and ore veins are often produced by multiple intrusions of reacting fluids into a porous soil, they studied the dissolution

invasions of corroding, dissolving, or melting fluids into a strongly heterogeneous substrate^{17–19}—slowly consolidating matrix fractal patterns are created that reflect the material's history.

Given this, Araújo and his colleagues developed a model of multiple invasion to simulate how these patterns form and how their fractal dimension changes.¹⁴ In this model, the first invasion occurs within a short time (geologically speaking) and leaves behind a certain damaged region. Slowly, the material is again strengthened (through, for example, crystallization or other chemical processes) partly repairing the damaged region. Then, suddenly, due to a tectonic mechanism such as an

earthquake or volcanic activity, another invasion occurs. It will favorably follow along the solid's weakest regions, which typically correspond to previously damaged regions. The goal is to understand to which degree this reinvasion will either fully or only partially coincide with the first invasion. Araújo and his colleagues calculated the invaded region's fractal dimension for different stages of the multiple invasion process. Their results reveal that the critical exponents vary as a function of the generation number G ; that is, they vary with the number of invasions. Finally, and more importantly, they show evidence that the fractal dimension of the invaded cluster changes from 1.887 ± 0.002 to 1.217 ± 0.005 . Thus, the multiple

we can view each person's trajectory as one decided on an entirely selfish basis—that is, on the existence of a possible optimal path (defined in terms of time and distance between home and work) in the absence of traffic.

If we now assume that this optimal path is unique and can accommodate only a finite flux of cars, we certainly expect a traffic jam somewhere along this special route. As a consequence, many people already en route will try to deviate from this traffic jam, while others who are continuously leaving their houses (and are fully aware of this situation) will try to follow a possible next-to-optimal path. Another traffic jam will then be generated and so on and so forth.

Once we determine the first optimal path connecting the lattice bottom and top, we search for its site with the highest energy. This becomes the first blocked site.

invasion process seems to display a continuous transition from the NTIP to the optimal path (under strong disorder) universality classes.

Optimal Path Cracks

A relevant application for optimal paths comes from a transportation network problem. Suppose that in a typical industrial city, a large fraction of the working population must, during every normal weekday, move by car from a residential zone to the city's industrial pole. To reach their work places, people must cross the city center (where most commercial establishments are located) through an intricate transportation network of streets, avenues, roads, and motorways. Following Wardrop's principle,²⁰

Two questions naturally arise from this daily problem:

- How and when will the transportation network eventually collapse?
- How will the network's topology and inhomogeneity affect its performance?

In a recent study, several of us provided a novel modelization for this complex problem that captures its essential features and offers insight on the statistical physics of these important questions.²¹ For completeness, we now describe this optimal path crack (OPC) model in detail.

The OPC substrate is a square lattice of size L with fixed boundary conditions at the top and bottom,

and periodic boundary conditions in the transversal direction. As noted earlier, we define the optimal path as the one among all paths connecting the lattice's bottom to its top with the smallest sum over all site energies. We introduce disorder in our model by assigning each site i an energy value $\varepsilon_i = \exp[\beta(p_i - 1)]$, where p_i is a random variable uniformly distributed in the interval $[0,1]$ and β is a positive control parameter. This transformation is equivalent to choosing ε 's values from the power-law distribution $P(\varepsilon_i) \sim 1/\varepsilon_i$ subjected to a maximum cutoff of $\varepsilon_{max} = \varepsilon^\beta$. Such a cutoff's existence makes the hyperbolic distribution normalizable for any finite value of β . Without losing generality, because we consider only positive p_i values, the Dijkstra algorithm becomes a suitable tool for finding the optimal path.²²

We form the OPC as follows. Once we determine the first optimal path connecting the lattice bottom and top, we search for its site with the highest energy. This becomes the first blocked site—that is, it can no longer be part of any path. This is equivalent to imposing an infinite energy on the site. Next, we calculate the optimal path among the lattice's remaining accessible sites, remove its highest energy site, and so on.

As Figure 1 shows, we continue the process iteratively until the system is disrupted and no remaining paths connect bottom to top. This would be analogous to the transportation system's complete collapse.

Figures 1a, 1c, and 1e show typical optimal paths generated at the beginning and end of the OPC process for $\beta = 1.0, 10$, and 100 , respectively. In Figure 1b, we can categorize the blocked sites that constitute the OPC in a typical random landscape generated under weak disorder conditions

$(\beta = 1.0)$ into three distinct types: the OPC's loopless backbone (blue), the multiple ends that dangle off it (red), and the network's numerous isolated clusters (black). As Figure 1d shows, moderate disorder conditions ($\beta = 10$) with a preserved OPC backbone substantially reduces the number of dangling ends and isolated clusters. Under very strong disorder ($\beta = 100$), only the OPC backbone remains (Figure 1f).

This behavior is closely related to the problem of minimum path in disordered landscapes.³ In the strong disorder regime, the minimum path's energy is controlled by a single site's energy. This situation occurs when we can't normalize the energy distribution—as in the case of a power-law distribution, $P(\varepsilon_i) \sim \{\varepsilon_i^{-\alpha}\}$, for $\alpha \leq 1$. The parameter β alone, however, doesn't determine the limit between weak and strong disorder, because system size is also a significant factor. More precisely, if β is sufficiently high, or the lattice size is sufficiently small, the distribution sampling near the cutoff region is less relevant. For any practical purpose, this network is considered in the strong disorder regime, resulting in a self-similar type of scaling for the minimum path. By increasing the network size, we might reach the point where we'd expect to start sampling larger energy values that are beyond the distribution's cutoff.

Above this scale, the system will return to the weak disorder regime, leading to a self-affine minimum path behavior; we'd thus expect an abrupt

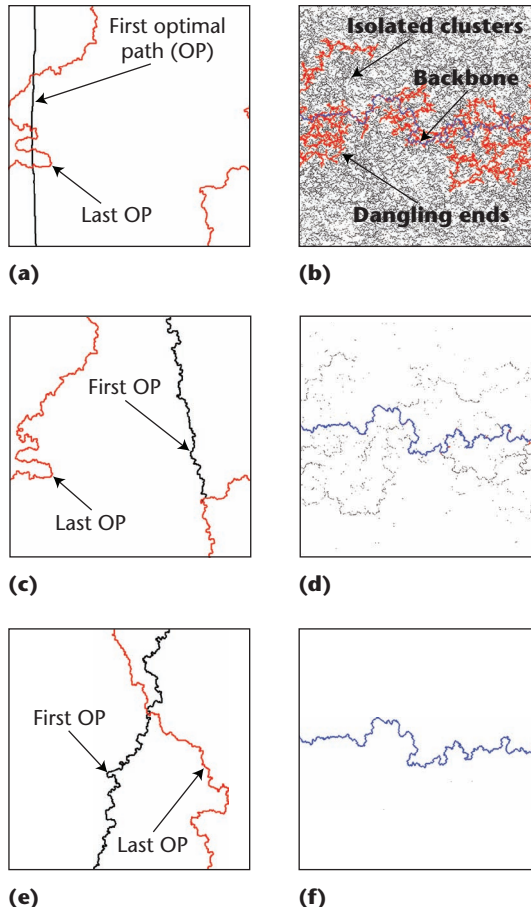


Figure 1. Typical realizations of the optimal path crack (OPC) model on a 512×512 lattice. In (a), (c), and (e), typical optimal paths generated at the beginning and end of the OPC process are shown for $\beta = 1.0, 10$, and 100 , respectively. (b) The resulting spatial distribution of blocked sites that constitutes the OPC in a typical random landscape generated under weak disorder conditions ($\beta = 1.0$). This OPC structure has three basic elements: the fracture's loopless backbone (blue), which effectively "breaks" the system in two; dangling ends (red); and isolated clusters homogeneously distributed over the entire network (black). The situation changes dramatically when the disorder parameter β 's value increases, as in (d), where the amount of dangling ends and isolated clusters in a OPC generated under moderate disorder conditions ($\beta = 6.0$) becomes significantly smaller than in the case of weak disorder. By increasing further the value of β , finally only the backbone remains, as in (f). Interestingly, this backbone is identical for all β values, while the entire set of blocked sites is highly dependent on how we introduce disorder into the system.

transition from the weak disorder regime, at small values of β , to the strong disorder regime, at large values of β .^{3,23}

Figure 2's inset shows that, for $\beta = 0.002$, the average mass of the OPC backbone scales is $M_b \sim L^{D_b}$, with an exponent $D_b = 1.22 \pm 0.02$. Once more, this exponent value is statistically identical to the fractal dimension previously found for the optimal path line under strong disorder.⁶ In this case, however, D_b 's value reflects a highly nonlocal system property that's intrinsically associated with the iterative process involved in the OPC calculation. As Figure 2 also shows, the OPC fracture's mass—which consists of both the backbone and its dangling ends—is in weak disorder. Although the crack itself grows as a power-law with size $M_f \sim L^{D_f}$ with an exponent $D_f = 1.59 \pm 0.02$, the total mass of blocked sites (crack and isolated clusters) is a constant fraction of the system's total mass—that is, $M_t \sim L^2$.

As Figure 2 shows, the results obtained for large values of β indicate that the stronger the system's disorder (low L or high β), the fewer the final blocked sites—that is, the OPC becomes increasingly localized in a singly connected crack line. Specifically, in the limit of very strong disorder, we find that only the OPC backbone mass M_b remains—that is, $M_t \rightarrow M_b$ and $M_f \rightarrow M_b$ —scaling in the same way as in the weak disorder limit ($M_b \sim L^{D_b}$, with $D_b = 1.22 \pm 0.02$).

Fractal Watersheds

A watershed line is another example in which the system's self-similar

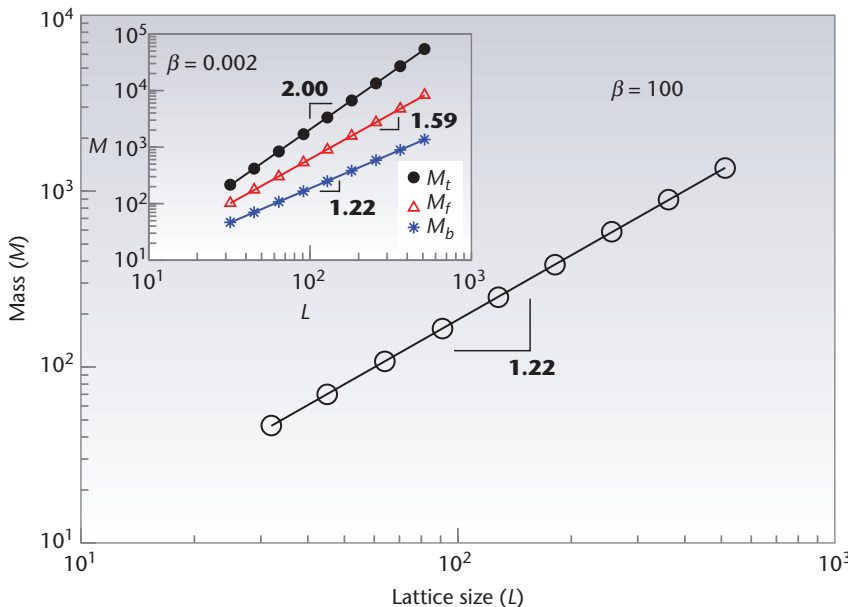


Figure 2. The effect of disorder on the optimal path crack (OPC) model’s geometry from simulations with 1,000 realizations of lattices and sizes varying in the range of $32 \leq L \leq 512$. Logarithmic dependence on the size L of the mass of all blocked sites M_t (circles) forming the OPC, the cluster of all sites in the fracture M_f (triangles), and the backbone mass M_b of the OPC that divides the system in two (stars) for $\beta = 0.002$. We consider the system in the weak disorder regime for this value of β and this range of system sizes. The three solid lines are the least-squares fits to the data of power-laws, $M_t \sim L^{D_t}$, $M_f \sim L^{D_f}$, and $M_b \sim L^{D_b}$, with exponents $D_t = 2.00 \pm 0.01$, $D_f = 1.59 \pm 0.02$, and $D_b = 1.22 \pm 0.02$, respectively. The inset shows the log-log plot of the masses M_t (circles), M_f (triangles) and M_b (stars) against system size L for $\beta = 6.0$. For this intermediate value of β , we can clearly identify the crossover from strong to weak disorder depending on the system scale. For small lattices, the system operates under strong disorder conditions. As a consequence, most of the blocked sites lie on the fracture path and the three masses M_t , M_f , and M_b are identical. As the system size increases, we reach the weak disorder regime and the three curves split apart. At larger scales, we should recover the same power-law behaviors found for sufficiently low values of β , as the main plot shows.

signature seems to fall in the same universality class as optimal paths in the strong disorder limit. Watersheds dividing adjacent water systems flowing into different seas have been used since ancient times to delimit boundaries. Border disputes between countries—such as between Argentina and Chile²⁴—have shown the importance of fully understanding a watershed’s subtle geometrical properties.

The watershed concept arises naturally in geomorphology, where it plays a fundamental role in areas such as water management, landslide, and flood prevention. Moreover, important applications can also be found in seemingly unrelated areas such as image processing and medicine. Slight

modifications of landscapes can produce large changes in the watershed and the effects can be highly nonlocal. Geographers and geomorphologists have studied watersheds extensively, but preliminary claims about fractality²⁵ have been restricted to small-scale observations and are therefore inconclusive. Despite the far-reaching consequences of scaling properties on watershed-related hydrological and political issues, researchers have dedicated few detailed numerical or theoretical studies to this subject.

Traditional cartographical methods for basin delineation have relied on manual estimation from iso-elevation lines and required considerable guesswork. Modern procedures are based upon

automatic processing of digital elevation map (DEM) or grayscale digital images, where gray intensity is transformed into height. A highly popular algorithm for watershed determination²⁶ uses rather complicated data structures and several passes over all pixels to calculate watersheds and is adequate for grayscale images (that is, for integer-height spaces). In a recent study, Eric Fehr and his colleagues investigated natural and synthetic watershed topology using novel numerical algorithms with highly improved efficiency.²⁷ Their results show that watersheds generated on large (10^8 sites) uncorrelated random landscapes are self-similar with fractal dimension $D_w = 1.211 \pm 0.001$. Once more, the exponent is close to the fractal dimension of optimal paths under strong disorder. We now show how one of Fehr’s two algorithms (the most efficient one) can calculate fractal watersheds.

First, let’s consider a DEM with sites i having heights b_i . For $k = 0, 1, \dots, N_{\text{sink}}$, let sink S_k be the subset of the lattice sites, which have their heights at the minimal possible value (such as equal to zero). These sinks are the terrain’s natural water outlets (such as an ocean). We consider that, at each time step, water slowly flows to the lowest-lying site on a flooded region’s perimeter. If, when starting from i , sink S_k is flooded before any other, then we assign site i to sink S_k ’s *catchment basin*. Clearly, this procedure introduces a lattice sites classification because it subdivides the system into non-overlapping subsets whose union is the entire lattice. Watersheds are precisely the lines separating neighboring basins.

In Fehr and colleague’s *IP-based algorithm*,²⁷ a cluster starts from site i and (like IP) grows by adding, at each

step, the smallest-height site on its perimeter until the first sink is reached. As Figure 3 shows, by noting that all sites occupied by a cluster when the sink is reached also drain to that sink, Fehr and colleagues devised a much more efficient procedure that visits each site only once and can be easily implemented. Their IP-based algorithm is fast enough to let us determine watersheds on lattices comprising 10^8 sites using a few CPU seconds on a workstation. In addition, the researchers calculated natural watersheds from landscapes of mountainous regions such as the Alps and Himalayas. They showed that these watersheds also display self-similarity, but with slightly smaller fractal dimensions— $D_w^A = 1.10 \pm 0.01$ and $D_w^{Hi} = 1.11 \pm 0.01$ in the Alps and Himalayas, respectively. They then explained the differences between the fractal dimensions by the presence of long-range correlations in real systems.

As our brief literature review shows, the fractal dimension of an optimal path in the strong disorder limit often appears in statistical physics models and therefore might represent a fundamental property for many different natural systems. To emphasize this common behavior and further support our hypothesis that all such systems fall in the same universality class, we presented three recent model applications in statistical physics; however, additional work in 3D and higher dimensions are needed to numerically confirm our hypothesis.

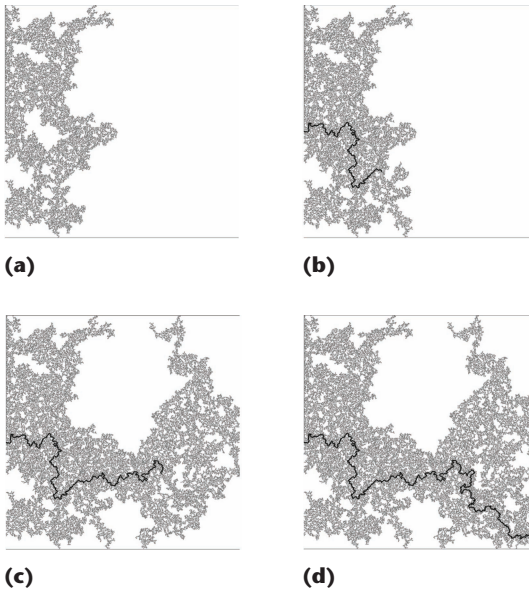


Figure 3. Three snapshots obtained at different stages from the invasion percolation (IP) algorithm developed by Eric Fehr and his colleagues to determine a typical watershed line (light gray) on an uncorrelated random landscape.²⁷ The algorithm visits only the sites in black; like IP, it starts a cluster from site i and grows it by adding, at each step, the smallest-height site on its perimeter until the first sink is reached. This procedure is somehow related to Prim's algorithm for growing minimum spanning trees (MST).⁸ The process is rather inefficient because, in principle, a new cluster must be grown from each site i . Noting that all sites occupied by a cluster when the sink is reached also drain to that sink, Fehr and his colleagues devised a more efficient algorithm that visits each site only once.²⁷ An additional modification permits an even more efficient algorithm. First, we test a line of points connecting two oceans by growing a cluster from each of them and determining where the drainage direction changes. This identifies a point of the water divide. Afterward, we test only points in that divide's vicinity. This procedure's advantage is that there are typically large parts of the terrain that the algorithm doesn't need to visit to determine the entire divide.

Acknowledgments

We thank the Brazilian agencies Coordenação de Aperfeiçoamento de Pessoal de Nível Superior (CAPES), Conselho Nacional de Desenvolvimento Científico e Tecnológico (CNPq), Fundação Cearense de Apoio ao Desenvolvimento Científico e Tecnológico (FUNCAP) and Financiadora de Estudos e Projetos (FINEP), and the Eidgenössische Technische Hochschule (ETH) Competence Center for “Coping with Crises in Complex Socio-Economic Systems”

(CCSS) in Switzerland for financial support.

References

- M. Mezard et al., “Nature of the Spin-Glass Phase,” *Physical Rev. Letters*, vol. 52, no. 13, 1984, pp. 1156–1159.
- S. Kirkpatrick and G. Toulouse, “Configuration Space Analysis of Traveling Salesman Problems,” *J. Physique*, vol. 46, no. 8, 1985, pp. 1277–1292.
- M. Cieplak, A. Maritan, and J.R. Banavar, “Optimal Paths and Domain Walls in the Strong Disorder Limit,” *Physical Rev. Letters*, vol. 72, no. 15, 1994, pp. 2320–2323.
- S. Havlin et al., “Optimal Path in Random Networks with Disorder: A Mini Review,” *Physica A*, vol. 346, no. 1, 2005, pp. 82–92.
- D. Stauffer and A. Aharony, *Introduction to Percolation Theory*, Taylor and Francis, 1994.
- N. Schwartz, A.L. Nazaryev, and S. Havlin, “Optimal Path in Two and Three Dimensions,” *Physical Rev. Letters*, vol. 58, no. 6, 1998, pp. 7642–7644.
- M. Cieplak, A. Maritan, and J.R. Banavar, “Invasion Percolation and Eden Growth: Geometry and Universality,” *Physical Rev. Letters*, vol. 76, no. 20, 1996, pp. 3754–3757.
- R. Dobrin and P.M. Duxbury, “Minimum Spanning Trees on Random Networks,” *Physical Rev. Letters*, vol. 86, no. 22, 2001, pp. 5076–5079.
- D. Wilkinson and J.F. Willemsen, “Invasion Percolation: A New Form of Percolation Theory,” *J. Physics A*, vol. 16, no. 14, 1983, pp. 3365–3369.
- P. Bak, C. Tang, and K. Wiesenfeld, “Self-Organized Criticality: An Explanation of the 1/f Noise,” *Physical*

- Rev. Letters*, vol. 59, no. 4, 1987, pp. 381–384.
11. A.P. Sheppard et al., "Invasion Percolation: New Algorithms and Universality Classes," *J. Physics A*, vol. 32, no. 49, 1999, pp. 521–529.
 12. M. Porto et al., "Optimal Path in Strong Disorder and Shortest Path in Invasion Percolation with Trapping," *Physical Rev. Letters*, vol. 79, no. 21, 1997, pp. 4060–4062.
 13. S. Schwarzer, S. Havlin, and A. Bunde, "Structural Properties of Invasion Percolation with and without Trapping: Shortest Path and Distributions," *Physics Rev. E*, vol. 59, no. 3, 1999, pp. 3262–3269.
 14. A.D. Araújo, J.S. Andrade, and H.J. Herrmann, "Multiple Invaded Consolidating Materials," *Physics Rev. E*, vol. 70, no. 6, 2004, 066150; <http://pre.aps.org/pdf/PRE/v70/i6/e066134>.
 15. E. Luijten, H.W.J. Blöte, and K. Binder, "Crossover Scaling in Two Dimensions," *Physics Rev. E*, vol. 56, no. 6, 1997, pp. 6540–6556.
 16. E. Salmon, M. Ausloos, and N. Vandewalle, "Aging of Porous Media Following Fluid Invasion, Freezing, and Thawing," *Physics Rev. E*, vol. 55, no. 6, 1997, pp. 6348–6351.
 17. M.T. Einandi, "6-km Vertical Cross Section Through Porphyry Copper Deposits, Yerington District, Nevada: Multiple Intrusions, Fluids, and Metal Sources," Int'l Exchange Lecture, Soc. Economic Geologists, June 1994; <http://pangea.stanford.edu/research/ODEX/marco-yingerton.html>
 18. B.J. Wanamaker, T.F. Wong and B. Evans, "Decrepitation and Crack Healing of Fluid Inclusions in San Carlos Olivine," *J. Geophysical Research*, vol. 95, no. B10, 1990, pp. 15623–15641.
 19. D.L. Turcotte, *Fractals and Chaos in Geophysics*, Cambridge Univ. Press, 1992.
 20. H. Youn, M.T. Gastner, and H. Jeong, "Price of Anarchy in Transportation Networks: Efficiency and Optimality Control," *Physical Rev. Letters*, vol. 101, no. 12, 2008; doi:10.1103/PhysRevLett.101.128701.
 21. J.S. Andrade et al., "Fracturing the Optimal Paths," *Physical Rev. Letters*, vol. 103, no. 22, 2009; doi:10.1103/PhysRevLett.103.225503.
 22. E.W. Dijkstra, "A Note on Two Problems in Connexion with Graphs," *Numerische Mathematik*, vol. 1, 1959, pp. 269–271.
 23. M. Porto et al., "Optimal Paths in Disordered Media: Scaling of the Crossover from Self-Similar to Self-Affine Behavior," *Physics Rev. E*, vol. 60, no. 3, 1999, pp. R2448–R2451.
 24. Reports of Int'l Arbitral Awards, *The Cordillera of the Andes Boundary Case (Argentina, Chile)*, United Nations Treaty Collection, 2006; http://untreaty.un.org/cod/riaa/cases/vol_IX/29-49.pdf.
 25. S.P. Breyer and R.S. Snow, "Drainage Basin Perimeters: A Fractal Significance," *Geomorphology*, vol. 5, no. 1–2, 1992, pp. 143–157.
 26. L. Vincent and P. Soille, "Watersheds in Digital Spaces: An Efficient Algorithm Based on Immersion Simulations," *IEEE Trans. Pattern Analysis and Machine Intelligence*, vol. 13, no. 6, 1991, pp. 583–598.
 27. E. Fehr et al., "New Efficient Methods for Calculating Watersheds," *J. Statistical Mechanics*, vol. 2009, Sept. 2009, P09007; doi:10.1088/1742-5468/2009/09/P09007.
-
- José S. Andrade, Jr.**, is a professor in the Department of Physics Department of Universidade Federal do Ceará. His research interests include statistical physics, transport phenomena, and complex systems. Andrade has a PhD in chemical engineering from Universidade Federal do Rio de Janeiro. He is a member of the Brazilian Physics Society. Contact him at soares@fisica.ufc.br.
-
- Saulo D.S. Reis** is a PhD student in the Department of Physics at the Universidade Federal do Ceará. His research interests include statistical mechanics, percolation theory, and the structure and functionality of complex networks. Reis has an MS in physics from Universidade Federal do Ceará. Contact him at saulo@fisica.ufc.br.
-
- Erneson A. Oliveira** is a PhD student in the Department of Physics at the Universidade Federal do Ceará. His research interests include fractals, the percolation process, and complex systems. Oliveira has an MSc in physics from Universidade Federal do Ceará. He is a member of the Brazilian Physics Society. Contact him at erneson@fisica.ufc.br.
-
- Eric Fehr** is a PhD student at the Institute of Building Materials at the Swiss Federal Institute of Technology (ETH) Zurich. His research interests include statistical properties of watersheds, corrections-to-scaling for high-precision estimates of scaling exponents, and cell migration in wound healing. Fehr has an MS ETH in theoretical physics from ETH Zurich. Contact him at ericfehr@ethz.ch.
-
- Hans J. Herrmann** is a professor at the Institute of Building Materials at the Swiss Federal Institute of Technology (ETH) Zurich. His research interests include statistical physics, computational physics, granular matter, and complex systems. Herrmann is a Guggenheim fellow, a member of the Brazilian Academy of Science, and a Max-Planck prize recipient. Contact him at hans@ifb.baug.ethz.ch.
-
- cn
Selected articles and columns from IEEE Computer Society publications are also available for free at <http://ComputingNow.computer.org>.

13
magazines

ARTIFICIAL INTELLIGENCE	BIO- TECHNOLOGY	SCIENTIFIC COMPUTING
COMPUTER HARDWARE	GRAPHICS & MULTIMEDIA	MULTIMEDIA INNOVATIONS
HISTORY OF COMPUTING	13 journals	DEADLINE 28 FEB 2011
HUMAN- CENTERED COMPUTING	IEEE Annals	IEEE
INTERNET & DATA TECHNOLOGIES	IEEE TRANSACTIONS ON AFFECTIVE COMPUTING	IT & SECURITY
MOBILE COMPUTING	IEEE TRANSACTIONS ON INFORMATION OVERLOAD	OPEN SOURCE
	IEEE TRANSACTIONS ON KNOWLEDGE AND DATA ENGINEERING	SOFTWARE
	IEEE TRANSACTIONS ON LEARNING TECHNOLOGIES	IEEE TRANSACTIONS ON PARALLEL AND DISTRIBUTED SYSTEMS
	IEEE TRANSACTIONS ON MOBILE COMPUTING	IEEE TRANSACTIONS ON SERVICES COMPUTING
	IEEE TRANSACTIONS ON NETWORKING	IEEE TRANSACTIONS ON SOFTWARE ENGINEERING
	IEEE TRANSACTIONS ON PERSPECTIVE DISPLAYS	SECURITY & PRIVACY

ONLINE PLUS™
publishing evolved

Three journals offer this new hybrid publishing model. Get online access, plus an abstract book and an interactive CD containing complete papers along with all of the supplemental files.

New in 2011



**IEEE Computer Society
Digital Library**

Includes access to all periodicals shown above and *Computer* magazine, plus over 3,800 conference publications.

**IEEE CS
DIGITAL
LIBRARY**

Order Full-Year subscriptions by 28 Feb 2011

NON-MEMBERS: Join IEEE Computer Society at www.computer.org/join for the best subscription rates. For non-member subscription rates, go to www.computer.org/portal/web/publications/nonmembersub

MEMBERS: You must renew your IEEE Computer Society membership for 2011 before ordering a subscription. Renew online at www.computer.org/nenewnow. Or call IEEE Customer Service +1 800 678 4333 ext. 2. For other promotion questions, email help@computer.org or call IEEE Computer Society at +1 800 272 6657 or +1 714 821 8380. Membership includes monthly issues of *Computer* magazine.

For fastest service, subscribe online at www.computer.org/portal/web/publications/membersub